Stem Cell Research (2012) 9, 59–68

Available online at www.sciencedirect.com

SciVerse ScienceDirect

www.elsevier.com/locate/scr

Proton-gated ion channels in mouse bone marrow stromal cells

Sandip Madhusudan Swain, Sreejit Parameswaran, Giriraj Sahu, Rama Shanker Verma, Amal Kanti Bera*

Department of Biotechnology, Indian Institute of Technology Madras, Chennai, 600036, TN, India

Received 16 November 2011; received in revised form 5 March 2012; accepted 30 April 2012
Available online 9 May 2012

Abstract A variety of ion channels like acid sensing ion channels (ASICs) and several members of the transient receptor potential (TRP) cation channel family are known to be activated by protons. The present study describes proton-gated current in mouse bone marrow stromal cells (BMSCs), by using whole cell patch clamp. Rapid application of extracellular solution of pH ≤ 6.5, evoked slow inactivating current with mean peak value of 328 ± 31 pA, (n = 25) at pH 5.0. The reversal potential was close to the theoretical Na^+ equilibrium potential, indicating that majority of the current is mediated by Na^+ and partially carried by Ca^{2+} as revealed by ion substitution experiments and Ca^{2+} imaging. ASICs blocker amiloride (1 mM) and nonselective cation channel blocker flufenamic acid (0.3 mM) reduced the current amplitudes by 36 ± 5% (n = 10) and 39 ± 7% (n = 14) respectively. Co-application of flufenamic acid and amiloride further decreased the current by 70 ± 7% (n = 7). However, capsazepine, SKF 96365 and ruthenium red had no effect. 10 mM of Ca^{2+} and 2 mM of La^{3+} inhibited the current by 39 ± 6% (n = 5) and 46 ± 6% (n = 4) respectively. Zn^{2+} (300 μM) and Gd^{3+} (500 μM) had no effect on the current amplitude. Low pH mediated cell death was completely inhibited by co-application of La^{3+} and amiloride. Reverse Transcriptase-PCR detected expression of mRNAs of ASICs and TRP family. In summary, our results demonstrate the functional expression of low pH-activated ion channels in mouse BMSCs.

Introduction

Mesenchymal stromal cells (MSCs) participate in wound healing, organ formation during development, and in tissue regeneration (Aicher et al., 2011). Some cells within cultured MSCs population can be differentiated into osteoblasts, chondrocytes and adipocytes (Liu et al., 2009; Leonardi et al., 2009). MSCs have the ability to home at the damaged site and promote tissue repair by releasing paracrine factors. Their immune modulatory properties make MSCs good candidates for preventing graft rejection and in autoimmune diseases (Zhao et al., 2010). MSCs can be isolated from various tissues. Bone marrow stromal cells (BMSCs) have been widely used in basic research as well as in regenerative medicine. However, little is known about the electrophysiological properties of BMSCs. To date, few ion channels have

Abbreviations: ASICs, Acid sensing ion channels; TRP, Transient receptor potential; TRPM7, Transient receptor potential melastatin type 7; BMSCs, Bone marrow stromal cells; FFA, Flufenamic acid; NMDG, N-methyl-D-glucamine.

* *Corresponding author*. Fax: +91 44 2257 4102.
E-mail address: amal@iitm.ac.in (A.K. Bera).

1873-5061/$ - see front matter © 2012 Elsevier B.V. All rights reserved.
doi:10.1016/j.scr.2012.04.005

been reported in mouse, rat and human BMSCs. Voltage gated delayed rectifying K^+ channels, TRPM7 channels, maxi K^+ channels, tetrodotoxin (TTX) sensitive sodium channels, and nifedipine sensitive calcium channels, have been reported to be present in different mesenchymal stem cells (Li and Deng, 2011; Cheng et al., 2010). Expression of low pH-activated channels like ASICs has not been reported in MCSs. In this study, we characterized the ionic current produced by low extracellular pH in mouse BMSCs. The importance of such proton activated channels in stromal cells has been discussed.

Results

Low pH-activated inward current

Rapid application of low pH solution generated fast inward currents that decayed slowly in BMSCs. 90% of the cells produced measurable currents in response to the application of acidic solutions of pH 4.0 to 6.5 (Fig. 1A). Interestingly, cells from the first 2 passages did not display these low pH evoked currents. The average current amplitude increased from passage numbers 3 to 9 and then remained constant till the 25th passage. At pH 5.0, the mean peak current was 328 ± 31 pA, (n = 25; holding potential −60 mV). At pH ≤ 5.0, about 8% of the cells showed rapid activation and inactivation followed by a slow sustained component, typical of ASIC3 (Fig. 1C). These cells were excluded from further characterization. The half-maximum activation pH (pH_{50}), as calculated from the dose–response curve, is about 5.0 (Fig. 1B).

Ion permeability

The current–voltage relationship (I–V) for current triggered by pH 5.0 is shown in Fig. 2. The reversal potential with 150 mM extracellular Na^+ and 30 mM intracellular Na^+ was 55 ± 6.6 (n = 7) [Fig. 2A], 14.1 mV higher than theoretical reversal potential calculated using the Nernst equation. In the presence of equimolar Na^+ in both extra and intra cellular solutions (30 mM), the reversal potential was 24.36 ± 7.6 mV (n = 4) [Fig. 2B], instead of "0" for the given solution as calculated using the Nernst equation. It indicates that the channels are permeable to other ions apart from Na^+.

Ca^{2+} is one of the major contributors of proton induced current generated by ASIC1a, TRPV1 and nonselective cation channels (Aarts et al., 2003; Xiong et al., 2004). When external Na^+ was substituted with equimolar concentration of NMDG, the peak current was reduced by 56 ± 4%, (n = 5) at pH 5.0 (Fig. 2C). Removal of both Ca^{2+} and Na^+ from the extracellular solution abolished the current almost completely (Fig. 2D), indicating that the observed inward current is due to both Na^+ and Ca^{2+}. We further examined the influx of Ca^{2+} by fura-2 ratiometric calcium imaging. Application of external solutions of pH 5.0 containing 2 mM Ca^{2+} transiently raised the intracellular calcium in most BMSCs. The florescence intensity

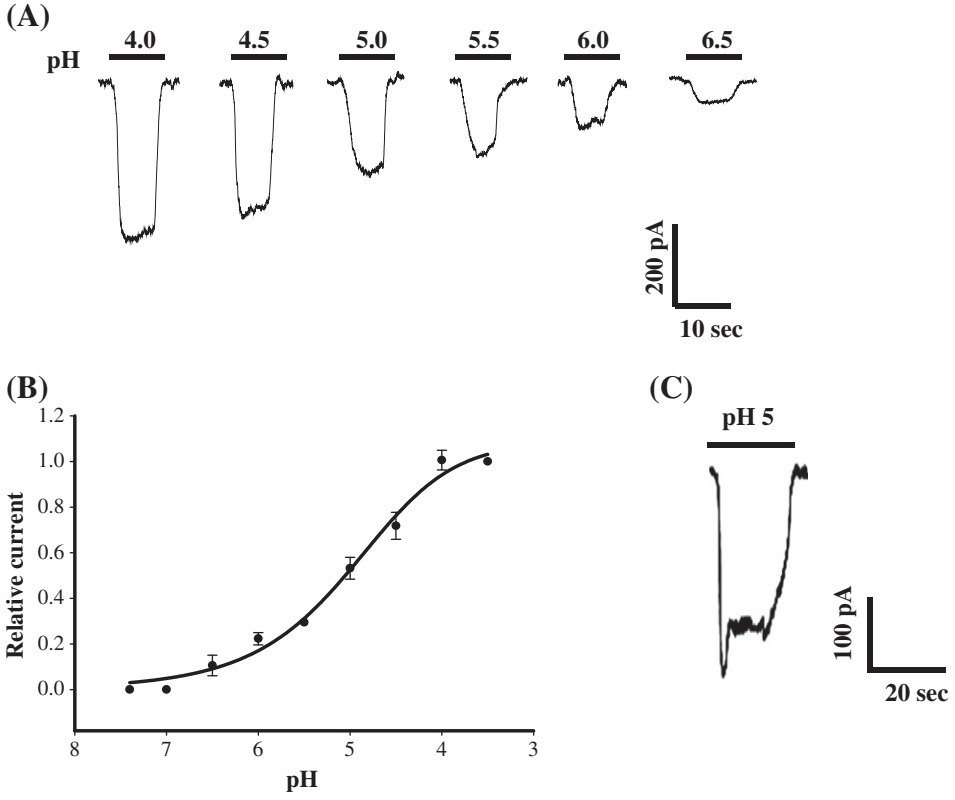

Figure 1 Low pH-activated current in MSCs. (A). Activation of inward currents in MSCs at different pHs. (B) pH dose–response curve was fitted to the Hill equation, as described in Materials and methods section. Each data point at different pH represents mean ± SEM obtained from 3 to 10 cells. The calculated pH_{50} was 4.97 ± 0.1. Current amplitude at a given pH was normalized to the current, induced by pH 3.5 (I/I_{pH} 3.5). (C) The representative trace showing a distinct biphasic current was observed in 8% of total cell population.

ratio (F_{340}/F_{380}) increased by 3.23±0.23 fold (n=30) [Figs. 2E and F]. Interestingly, low pH solution, devoid of Ca^{2+} also raised intracellular calcium to a lesser extent, indicating acid induced calcium release from intracellular stores (Fig. 2E).

To determine the order of permeability of different monovalent cations, the external Na^+ was replaced with equimolar concentration of different monovalent cations. The rank order of permeability was observed as $Na^+ > NH_4^+ > Li^+ > Cs^+ > NMDG$, as calculated from the peak currents before and after substitution of the Na^+ with respective monovalents (Fig. 3). When external Ca^{2+} was substituted with 4 mM of Ba^{2+} the peak current amplitude at pH 5.0 did not differ significantly (Fig. 3).

Pharmacologic properties of low pH induced inward current

Low pH can activate several types of channels and the observed inward current could be due to the cumulative effect of all such activated channels. The possible activated channels could be ASICs, and some members of the sub-family of TRP channel. We used several known blockers of ASICs and TRP channels for further characterization. Amiloride (1 mM), a nonspecific blocker of ASICs (Lingueglia et al., 1997), inhibited the peak current at pH 5.0 by 36±5% (n=10) [Figs. 4A and C]. About 70% of the cell population was sensitive to amiloride. To determine the functional expression of different ASIC isoforms, we used metal ions like Ni^{2+}, Cd^{2+} and Zn^{2+}, which are known to modulate ASICs in a subtype specific manner. Application of Ni^{2+} (100 μM) resulted in the reduction of current amplitude by 13±4% (n=6) (Fig. 4A). Ni^{2+} has been reported to block homomeric ASIC1a and heteromeric ASIC1a/2a channels without affecting ASIC1b, 2a, and ASIC3 homomeric channels. However, Ni^{2+} does not block the ASIC1a/3 and 2a/3 heteromeric channels (Staruschenko et al., 2007). Since, 36±5% of proton activated current was contributed by ASICs (amiloride sensitive), 13% attenuation of peak current by Ni^{2+} reflects that about 1/3 of expressed ASICs (homomeric ASIC1a and heteromeric ASIC1a/2a) were sensitive to Ni^{2+}. However, Cd^{2+} (100 μM) and Zn^{2+} (300 μM) had no effect on current amplitude (Fig. 4A). Cd^{2+} is known to inhibit ASIC2a and ASIC3 homomeric channels as well as ASIC1a/2a, 1a/3, and 2a/3 heteromeric channels but not the ASIC1a homomeric channel (Staruschenko et al., 2007.) Zn^{2+} has been reported to potentiate ASIC2a containing channels (Baron et al., 2001). These results suggest that, ASIC1a homomeric channel is the major ASIC, expressed in BMSCs.

Besides ASICs, some TRP channels also are known to be activated at low pH (Peter, 2007; Sugiura et al., 2007). Several blockers were used to identify the different TRP members, which can be activated by proton in MCSs. Ruthenium red (5 μM), a nonspecific blocker of TRPV channels (TRPV1–V6) (Clapham, 2003) and TRPM6 (Voets et al., 2004), had no effect on low pH-induced current. La^{3+} and Gd^{3+} differentially modulate most of the TRP channels including TRPM2, TRPM3 and TRPM7 (Clapham, 2003; Grimm et al., 2005). 1 mM and 2 mM La^{3+} inhibited low pH-induced current by 26±7% (n=5) and 46±6% respectively (Figs. 4A and B). However, Gd^{3+} (1 mM) had no such effect on low pH-induced current (Fig. 4A). Interestingly, TRPV1 blocker capsazepine (20 μM) (Bevan and Szolcsányi, 1990) and SKF96365 (100 μM) (1-(beta-[3-(4-methoxy-phenyl) propoxy]-4-methoxyphenethyl)-1H-imidazole hydrochloride), a blocker of TRPC sub-family and receptor mediated calcium entry (RMCE) (Bomben and Sontheimer, 2008; Romero-Mendez et al., 2008) did not affect the proton activated current (Fig. 4A). However, the current was significantly reduced by nonselective cation channel blocker, flufenamic acid (FFA) [Fig. 4], which is known to block several TRP members, including TRPC3, TRPC5, TRPM2, TRPM4 and TRPM5 (Albert et al., 2006; Ullrich et al., 2005). Proton activated current was reduced significantly, when BMSCs were preconditioned with FFA (50 μM) (Fig. 4D). Prolonging pre-conditioning time enhanced the efficacy of FFA. When the cells were treated with FFA (50 μM) for 5 s, 30 s and 50 s the current amplitude decreased by 5.8±4% (n=4), 41.3±7.9% (n=5) and 62.6±11% (n=4) respectively (Fig. 4D). Further inhibition was not observed by prolonging the application time. FFA also blocked the current when co-applied with the low pH external solution. FFA (300 μM) reduced the peak current by 39±7.3% (n=14) at pH 5.0 (Figs. 4A and C). Full recovery of the current was not observed after 3 min of washing. Co-application of FFA (300 μM) and amiloride (1 mM) further reduced the current by 70±6% (n=7) [Fig. 4C]. To know the subtype of TRP channels that actually contributes to the low pH evoked currents, we generated a current–voltage relationship plot (I–V plot) at pH 4.0, after blocking ASICs with 1 mM amiloride. In response to voltage ramps of 50 ms duration spanning −100 to +100 mV, cells produced robust outward rectifying currents and little inward currents (Fig. 4E). Such an I–V curve is characteristic of the TRPM7 channel (Nadler et al., 2001).

Effect of extracellular calcium

Extracellular calcium modulates various ion channels, including ASICs (Immke and McCleskey, 2003; Paukert et al., 2004). The effect of extracellular calcium on proton induced current in BMSCs was studied. In the presence of 5.0, 10 and 20 mM calcium, the peak current reduced by 21±6% (n=6) 30±6% (n=7) and 35±9% (n=5) respectively (Fig. 5). 1.0 and 2.0 mM Ca^{2+} showed a similar trend.

Reverse transcriptase polymerase chain reaction (RT-PCR)

RT-PCR was used to assess the gene expression of various low pH-activated channels in BMSCs. cDNAs synthesized from total RNA was used for the amplification of desired genes along with mouse specific primers (Table 1). Fig. 6, shows the expression profile of the various studied genes. ASIC1a, ASIC3, TRPV1 and TRPM7 showed robust amplification and the fragment sizes were as expected. However, ASIC1b and ASIC2a were not detected even by amplification with multiple primer pairs from the different sites of the coding region.

Proton-gated channels are associated acid induced cell death

Over-activation of proton activated channels is known to cause cell death by increasing intracellular calcium (Chu and Xiong, 2012; Bae and Sun, 2011). We examined the role of proton-gated channels in low pH-induced cell death. About 20% of the cells died when BMSCs were exposed to

extracellular solution of pH 6.0 for 1 h. Interestingly there was no significant cell death when proton activated channels were blocked with La^{3+} and amiloride (Fig. 7), suggesting that these channels are indeed associated with acid induced cell death of BMSCs. Although FFA reduced the channel current significantly, we could not use it in cell death assays due to its cytotoxic effect.

Discussion

In the last decade, BMSCs have gained considerable attention due to their immense potential in regenerative therapy. Although ample work on different receptors and signaling pathways has been published, there are hardly any studies on ion channels expressed in BMSCs. Recent studies have demonstrated that multiple ion channels are heterogeneously present in MSCs and the patterns and phenotypes of ion channels are species- and/or origin-dependent (Li and Deng, 2011). In the present study, we report the functional expression of low pH-activated channels in mouse BMSCs. By systematic use of different channel modulators/blockers, we demonstrated that BMSCs express ASICs and TRP channels that are activated by low pH. The electrophysiological data were further substantiated by RT-PCR. About 36% of low pH-induced current was contributed by amiloride sensitive ASICs. The rest of the current was due to the activation of TRP channels.

mRNAs of ASIC1a and ASIC3 were detected in BMSCs (Fig. 6). Although, RT-PCR analysis demonstrated robust amplification of ASIC3, only 8% of cells showed typical ASIC3 type whole cell current (Fig. 1C). Besides, we also demonstrated that homomeric ASIC1a is predominantly expressed in BMSCs. The possibility of functional heteromeric channel containing ASIC1a and ASIC3 can be ruled out since Cd^{2+} failed to inhibit the current.

Blocking of ASICs by increased concentration of extracellular Ca^{2+} is a well known phenomenon. It has been hypothesized that Ca^{2+} occludes the channel pore and protonation of several negatively charged amino acids in the extracellular domain causes the opening of ASIC by reliving the Ca^{2+} block. It has also been proposed that Ca^{2+} may inhibit ASICs by modulating the gating (Immke and McCleskey, 2003; Paukert et al., 2004). We showed that

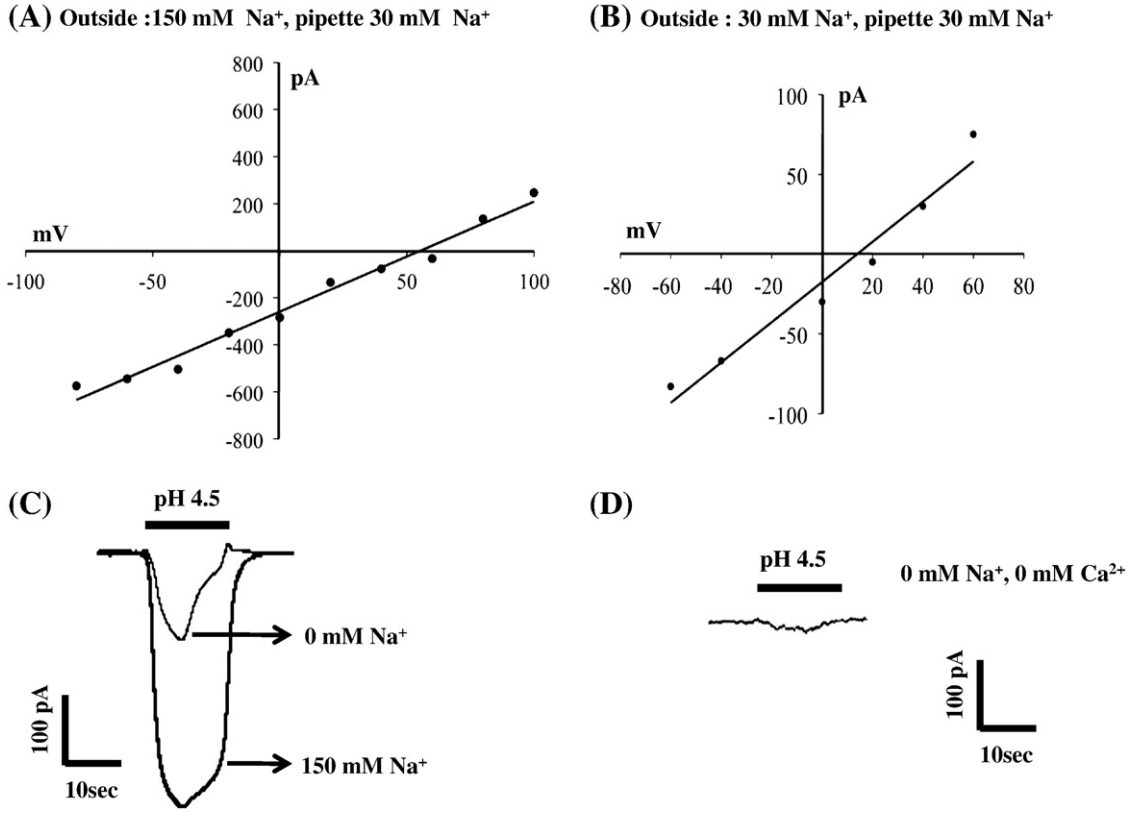

Figure 2 Na^+ selectivity and Ca^{2+} permeability of low pH-activated channels in MSCs. (A and B) Current–voltage (I–V) relationships of proton-gated channels at different extracellular Na^+ concentrations. (A) Reversal potential, calculated from I–V plot at outside [Na^+] 150 mM and inside [Na^+] 30 mM was 55.4 ± 6.6 mV (n = 7), which is higher than the reversal potential of the theoretical Na^+ equilibrium potential. (B) Reversal potential decreased to 24.36 ± 7.6 mV, (n = 4) by reducing external Na^+ concentration to 30 mM. (C) Substitution of extracellular Na^+ with equimolar NMDG reduced the current amplitude by 56 ± 4%, (n = 5). (D) Complete removal of extracellular Na^+ and Ca^{2+} abolished 95 ± 4% (n = 4) of the currents, measured at pH 4.5. (E and F) Representative F340/F380 ratio and images showing low pH-induced intracellular Ca^{2+} rise in MSCs. F340/F380 ratio increased by 3.23 ± 0.23 fold (n = 30), upon application of extracellular solution of pH 5.0. Removal of Ca^{2+} from extracellular solution reduced the Ca^{2+} rise significantly ($p < 0.01$). F340/F380 ratio increased by 1.46 ± 0.1 fold (n = 30) in the absence of extracellular Ca^{2+}. (F) Representative fluorescent images of cells loaded with fura-2 are taken at 340 nm of excitation before (pH 7.4) and after application of low pH solution.

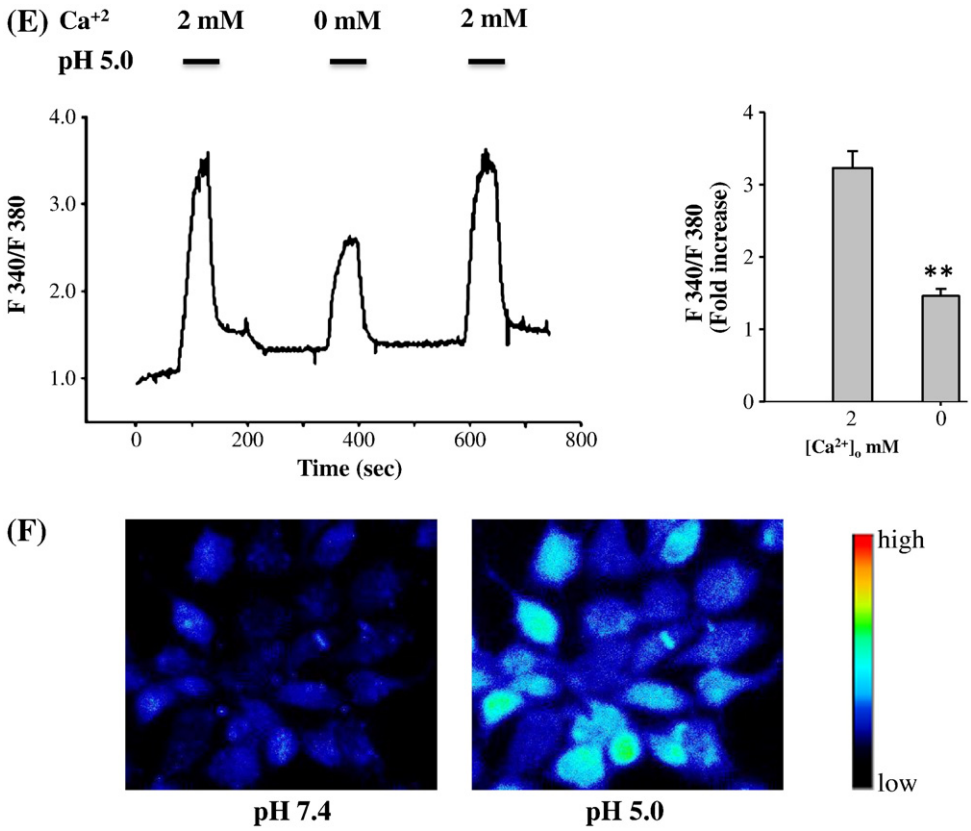

Figure 2 (*continued*).

elevated concentrations of extracellular Ca^{2+}decreased low pH-induced current (Fig. 5). Although statistically significant inhibition was observed with 10 mM and 20 mM Ca^{2+}, the trend was evident with even 1.0 and 2.0 mM Ca^{2+}. ASICs contributed only 36% of the total current and therefore even a slight inhibition by Ca^{2+} indeed reflects a larger change in ASIC currents.

About 64% of low pH-induced current was due to the activation of FFA sensitive TRP channels. The expression of TRPV1 and TRPM7 was particularly determined since they were known to be activated by low pH. TRV1 is directly gated by proton whereas, low pH strongly potentiates TRPM7 (Jiang et al., 2005; Gunthorpe et al., 2002). RT-PCR analysis detected the presence of both TRPV1 and TRPM7 mRNAs (Fig. 6). A major problem associated with TRP channel research is the lack of specific pharmacological agents and therefore, we had used nonspecific blockers as well as fairly specific blockers to identify the functional TRP channel subtypes. Although TRPV1 mRNA was detected in BMSCs, it does not seem to contribute low pH-activated current since a potent antagonist, capsazepine, failed to attenuate the current (Fig. 4A). Besides Gd^{3+}, that generally potentiates TRPV1, (Tousova et al., 2005) had no effect on the current (Fig. 4A). These data suggests that although undifferentiated BMSCs express TRPV1 mRNA, functional expression is limited. The TRPV1 functional channel may appear after differentiation of BMSCs into a specific cell type. Another TRP family member, TRPC5, was also reported to be activated at low pH (Semtner et al., 2007). La^{3+} and Gd^{3+}, which potentiate TRPC5, (Semtner et al., 2007) had inhibitory and no effect on the proton activated current respectively. Thus, the involvement of TRPC5 can be ruled out. Acidic pH can

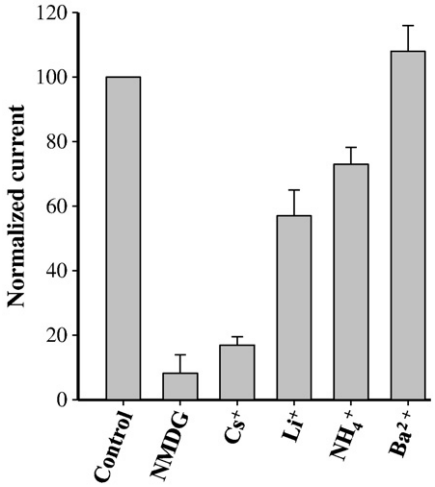

Figure 3 Cation permeability of low pH-activated channels in MSCs.Permeability of different monovalent cations was tested by substituting external Na^+ with equimolar concentration of different monovalent cations. Average peak current induced by pH 5.0 in 150 mM external Na^+ (control) was normalized to 100. Currents with different substituted cations are expressed as 'relative to control'. Among the tested cations, NH_4^+ showed highest permeability after Na^+ and NMDG the lowest. Replacement of extracellular Ca^{2+} with 4 mM Ba^{2+} had no significant effect on current amplitude.

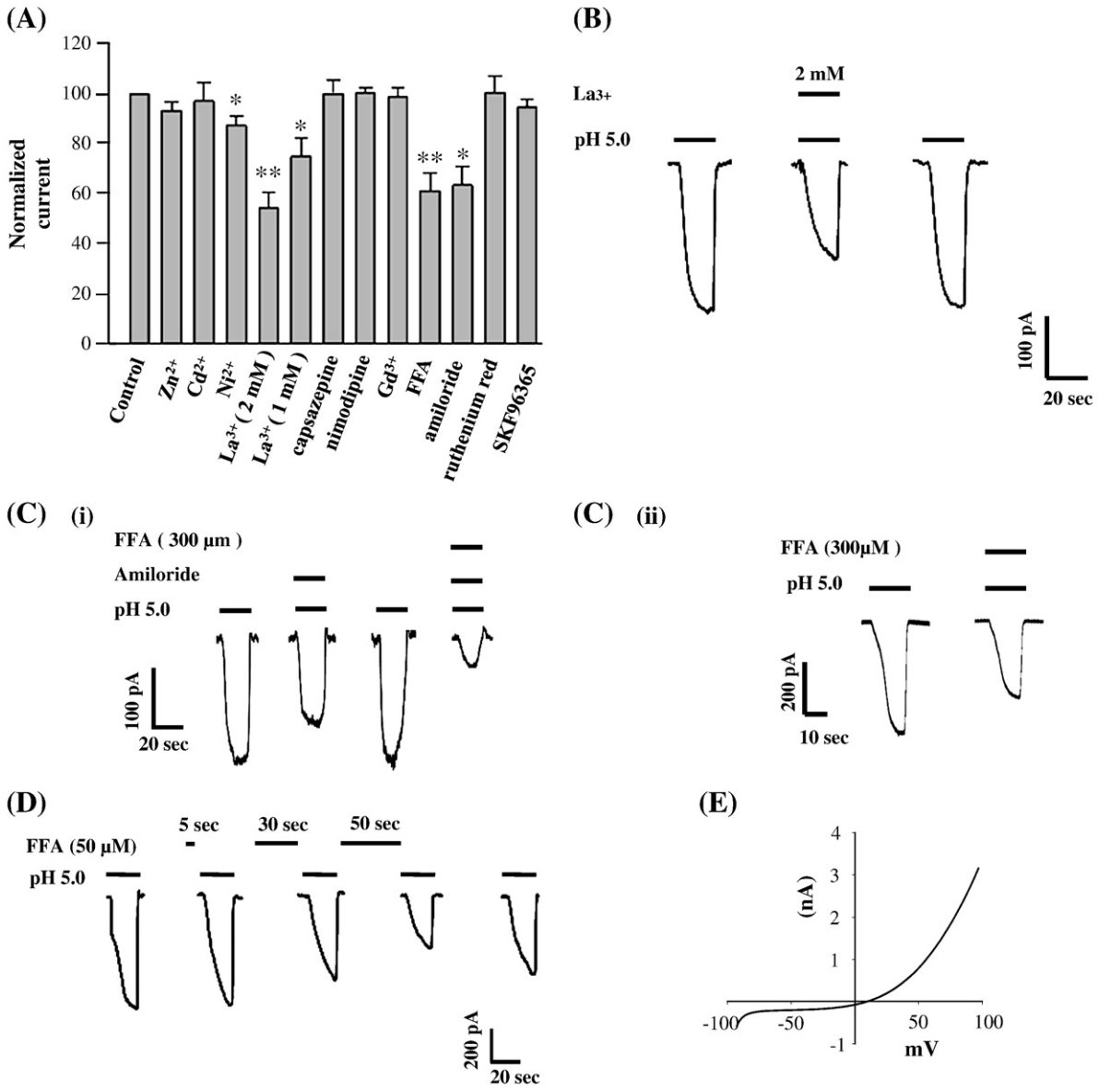

Figure 4 Inhibition of low pH-activated channels in MSCs by different ions and pharmacological agents. (A) Low pH-activated currents were reduced significantly by 1 mM amiloride, 300 μM flufenamic acid (FFA), and both 1 mM and 2 mM La^{3+}. Metal ion Ni^{2+} reduced the current by 13 ± 4% (n = 6), whereas Zn^{2+} and Cd^{2+} had no significant effects. Other blockers like SKF 96365, ruthenium red, gadolinium, nimodipine and capsazepine did not alter the current significantly. (B and C) Traces represent the inhibition of currents by La^{3+} and amiloride in combination with FFA. Co-application of amiloride and FFA blocked the current by 69.48 ± 6.57%, n = 7 ($p < 0.05$). (C-ii) Represents effect of FFA alone. Current traces presented in (C-i) and (C-ii) are recorded from two different cells. (D) 50 μM of FFA blocked the channel current by 5.8 ± 4% (n = 4), 41.3 ± 7.9% (n = 5) and 62.6 ± 11% (n = 4), when preconditioned at closed state for 5 s, 30 s and 50 s respectively. (E) Current–voltage relationships in the presence of amiloride, obtained from BMSC at pH 4.0. The currents exhibited strong outward rectification with insignificant inward component, a characteristic of TRPM7 channel.

potentiate the activity of TRPM7 by 10 fold (Jiang et al., 2005; Cui et al., 2011). It is also sensitive to FFA and La^{3+} (Jiang et al., 2003; Kerschbaum et al., 2003). Therefore, the FFA sensitive component of the low pH-activated current in BMSCs is possibly due to the activation of TRPM7 channels. To confirm it further, we generated an I–V plot at low pH in the presence of amiloride for blocking ASICs. As shown in Fig. 4E, the I–V plot shows outward rectification with slight inward current, a typical characteristic of the TRPM7 channel (Nadler et al., 2001).

TRPM7 channel has been implicated in cell survival and proliferation. In zebra fish, TRPM7 knockouts showed several development defects in skeletal muscle and growth retardation (Elizondo et al., 2005). TRPM7 was also reported to regulate cell migration (Wei et al., 2009). Knocking down TRPM7 in DT-40B cells resulted in growth retardation and death (Nadler et

al., 2001). Similarly, TRPM7 knocked down MSCs showed decreased cell proliferation and viability, suggesting its role in differentiation and development (Cheng et al., 2010). On the other hand, ASICs are yet to be implicated in cell proliferation or differentiation. Over-activation of ASICs and TRP channels is known to cause cell death by increasing intracellular calcium. They are associated with low pH-induced cell death in many patho-physiological conditions (Xiong et al., 2004; Bae and Sun, 2011). In our study, BMSCs showed TRP and ASICs mediated intracellular calcium rise and mortality, when treated with low pH solutions. Acid induced death was prevented by blocking these channels. In regenerative therapy, MSCs are often exposed to the inflammatory milieu where extracellular pH is invariably acidic (Nedergaard et al., 1991; Siesjo et al., 1996) and thus activation of these channels is inevitable. Therefore the viability of BMSCs in the affected region will be compromised unless activities of proton-gated calcium permeable ASICs and TRP channels are controlled.

Materials and methods

Reagents

All reagents for cell culture were purchased from Gibco Life Technologies, Grand Island, NY, USA. Fura-2AM was procured from Molecular Probes, Eugene, Oregon, USA. All channel blockers, BAPTA, NMDG, EGTA and salts used in the experiments were purchased from Sigma-Aldrich Corp., St. Louis, MO, USA.

Isolation and culture of bone marrow derived BMSCs

6–8 weeks-old Swiss albino mice were procured from Tamil Nadu Veterinary and Animal Sciences University, Chennai, India. The procedure was approved by the Institutional Animal Ethics Committee. Mice were euthanized and BMSCs were isolated as described earlier (Sreejit and Verma, 2011). Briefly, BMSCs were collected from the aspirates of the femurs and tibias of mice (~20 g) with 10 ml of MSC maintenance medium (MM) consisting of DMEM/F12 (1:1) supplemented with fetal calf serum (FCS) (20%), penicillin (100 U/ml), and streptomycin (100 mg/ml), 2 mM L-glutamine, 0.1 mM nonessential amino acids and 3 mM sodium pyruvate. Cells were washed twice and re-suspended in bone marrow matrix media (BMM) and plated at a density of 1×10^4 cells/cm^2 in flasks. Cultures were maintained at 37 °C in a humidified atmosphere containing 5% CO_2. After 72 h, nonadherent cells were discarded, and the adherent cells were thoroughly washed twice with Dulbecco's Phosphate Buffered Saline (DPBS). Fresh complete medium was added and replaced every 3 or 4 days for ~10 days. The cells were harvested after incubation with 0.25% trypsin and 1 mM EDTA for 5 min at 37 °C and re-plated at densities of 5×10^3 cells/cm^2. These cells were maintained for electrophysiological studies. Results presented here are from the cells between passages 7 and 13.

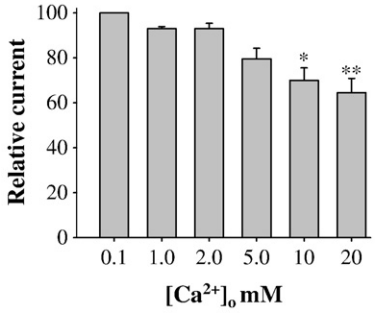

Figure 5 Effect of extracellular calcium.There was no significant change in peak current with 0.1, 1 and 2 mM extracellular Ca^{2+}. However in the presence of 5 mM, 10 mM and 20 mM calcium, the peak current reduced by 21±5.9% (n=6), 30±6.4% (n=7) and 35±8.9% (n=5) respectively.

Patch clamp recording

Low pH-activated whole cell current was recorded with amplifier Axopatch 200B (Molecular Devices, Sunnyvale, CA, USA), as described earlier (Jetti et al., 2010). Patch pipettes of 4–6 MΩ were prepared from borosilicate glass using pipette puller P-80 (Sutter Instrument Company, Novato, CA, USA). Current was recorded at a holding potential of −60 mV unless otherwise mentioned. Digidata 1440 and pClamp 10 (Molecular Devices, Sunnyvale, CA, USA) were used for digitization, data acquisition and analysis. Data were sampled at 10 kHz and low pass filtered at 1 kHz. The external solution contained (in mM): 150 NaCl, 5 KCl, 1 $MgCl_2$, 2 $CaCl_2$, 10 glucose and 10 HEPES (pH 7.4). The pipette solution for whole cell patch recording contained (in mM): 120 KCl, 30 NaCl, 1 $MgCl_2$, 0.5 $CaCl_2$, 0.5 EGTA, 2 Mg-ATP, and 10 HEPES (pH 7.2). 2-[N-morpholino] ethanesulfonic acid (MES) was used for buffering external solutions of pH below pH 6.0. The extracellular solutions without Na^+ or 30 mM Na^+ were prepared by substituting with equimolar *N*-methyl-D-glucamine (NMDG). 5 mM EGTA or 1 mM BAPTA was added in Ca^{2+}-free medium of pH 7.4 and pH<7.0 respectively. In the ion permeability experiment, the pipette solution contained (in mM) 120 CsCl, 30 NaCl, 1 $MgCl_2$, 0.5 $CaCl_2$, 0.5 EGTA, 2 Mg-ATP and 10 HEPES. In external solution, NaCl was replaced with 150 mM monovalent ion. The Cs^+ permeability experiment was performed with 120 mM KCl in pipette instead of 120 mM CsCl.

Ca^{2+} imaging

Intracellular calcium ($[Ca^{2+}]_i$) was measured by standard ratiometric method, using Fura-2. Cells grown on cover slips were incubated with 5 μM fura 2-AM in bathing solution containing (in mM): 150 NaCl, 5 KCl, 2 $CaCl_2$, 1 $MgCl_2$, 10 HEPES, and 10 glucose (pH 7.4) at room temperature (22–24 °C) for 30 min, followed by 30 min of washing with dye free solution. $[Ca^{2+}]_i$ was imaged with appropriate excitation and emission filters for fura-2. Images were captured with an Andor CCD camera (Andor Technology, Belfast, Northern Ireland, UK), attached to an Olympus IX71 inverted microscope. The low pH test solution was supplemented with major Ca^{2+} entry pathway blockers e.g. CNQX (20 μM, for glutamate receptors) and nimodipine (10 μM, for L-type calcium channel). Image intensity was calculated from the background subtracted images, by using Image J software.

Table 1 Mouse gene specific primers for RT-PCR.

Name	Gene Bank accession no.	Primer sequence (5′-3′ and F-forward, R-Reverse)	Product size, bp
ASIC1a	NM_009597.1	(Set-1), F: CTTGCCCACATCTTCTCCTATG R: AGTCCCACCTTTCATGGTCTTC	515 (a)
		(Set-2), F: CCTTCAACATGCGTGAGTTCTAC R:TGGTCTTTCTCCACTAGGAAGTC	616 (a*)
		(Set-3), F: GCCTATGAGATCGCAGGG R: AAAGTCCTCAAACGTGCCTC	286 (a)
ASIC1b	AB208022.1	Set-1), F: AGAATCGGAAGAAGAAGAAGAGAAG R: GTAGAGCAAGTCAGGGTAGCTGAG	328 (n)
ASIC2a	NM_001034013.2	(Set-1), F: TCGGAGAGAGTATCCTACTATTTCTCAT R: CTTCAAACGTTGTTTCCTCTGTCT	521 (n)
		(Set-2), F: CAACTTCAAACACTACAAACCGAAG R: CAGTAATTGCTGTCCTTTTCTGC	628 (n)
		(Set-3), F: GAAGAGGAAGGGAGCCATGAT R: GGCAGAAGTTCGCAATGTG	256 (n)
ASIC3	NM_183000.2	(Set-1), F: CTCTACCAGGTGGCTGAGCGGGTTC R: AGTTGTGCCATGTCAAAAGTCG	687 (a)
		(Set-2), F: GCTGAACATGCTGCCTACCTTC R: CTGGGCTGGCACAGTCCTTGT	404 (a*)
		(Set-3), F: CCCAGCTCTGGACGCTATG R: TCTTCCTGGAGCAGAGTGTTG	414 (a)
TRPV1	NM_001001445.1	(Set-1), F: AGACAGAGACCCTAACTCCAAGC R: AATGGCAATGTGTAATGCTGTC	571 (a*)
		(Set-2) , F: GTGGAGGTGGCAGATAACACAG R: GAAGAAGAAGTAGACTCCTCCTGACAC	533 (a)
TRPM7	NM_001164325.1	(SET-1), F: ATTCATGCTAGAATTGGGCAAG R: AGTGTAAGGATAAGCTGGTCAAATG	396 (a*)

Amplified (a), amplified and shown in Fig. 6 (a*) and not amplified (n).

Cell viability assay

Confluent BMSC cultures grown on 24 well plates were incubated with an extracellular solution of pH 6.0, with or without amiloride and Lanthanum chloride (300 μM each) for 1 h in a cell culture incubator (5% CO_2, 37 °C). The control group was treated with an extracellular solution of pH 7.4. After washing, cells were treated with 100 μg/ml Alamar blue prepared in serum and antibiotic free media at 37 °C for 2 h (Nakayama et al., 1997). Fluorescence intensity was measured with 570 nm excitation and 595 nm emission. The reduction of fluorescence intensity correlates with cell death. Fluorescence intensity of the cells treated with extracellular solution of pH 7.4 was normalized to 100% viability and other groups were expressed accordingly.

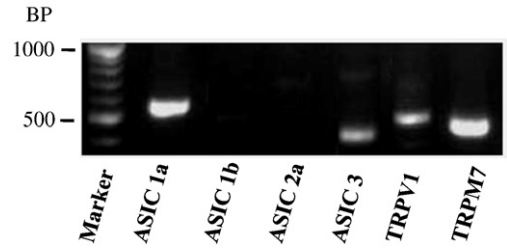

Figure 6 RT-PCR analysis.RT-PCR analysis detected messenger RNAs (mRNA) of ASIC1a, ASIC3, TRPV1 and TRPM7 in BMSCs. ASIC1b and ASIC2a were not detected. The gel-picture represents RT-PCR products of one set of primers of each gene.

RT-PCR

Total RNA of mouse bone marrow derived MCSs was isolated by using the acid guanidinium thiocyanate–phenol–chloroform extraction method (Chomczynski and Sacchi, 1987). RNA was subjected to cDNA conversion using M-MLV Reverse Transcriptase (New England Biologicals, Beverly, MA, USA) along with oligo (dT) primers. cDNA was then used for polymerase chain reaction (PCR) analysis with mouse ASICs and TRP channel primers made from coding sequence regions

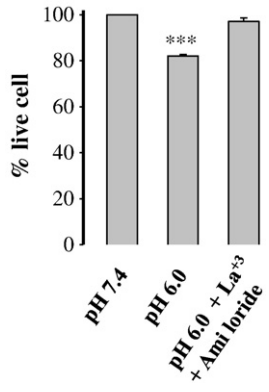

Figure 7 Blockers of ASICs and TRP channels protect BMSCs from acid induced death.Co-application of ASICs blocker amiloride and TRP channels blocker La^{3+} prevented low pH (pH 6.0, for 1 h)-induced death of BMSCs. Values are mean ± SEM of three independent experiments.

(Table 1). To determine the isoforms of ASICs and TRPV1, different sets of primer from different coding regions of mouse ASIC 1a, 2a, 3 and TRPV1 were used. cDNA was amplified using a DNA thermal cycler containing a standard concentration of PCR components and PCR products were observed in 1.5% Agarose gel in TAE buffer.

Statistical analysis

Recorded current was analyzed with Clamp fit 10.0 (Molecular Devices, Sunnyvale, CA, USA) and dose–response curves were fitted with the Hill equation to calculate IC_{50}, using Sigma plot 11.0. Statistical test was carried out by using Student's *t*-test for comparison of two groups and ANOVA for multiple comparisons.

Acknowledgments

This work was supported by the Department of Biotechnology and the Department of Science and Technology, India. Sandip M. Swain and Sreejit Parameswaran received doctoral fellowships from UGC and ICMR, India respectively. We acknowledge Divya and Mohona for their efforts in correcting the manuscript.

References

Aarts, M., Iihara, K., Wei, W.L., Xiong, Z.G., Arundine, M., Cerwinski, W., MacDonald, J.F., Tymianski, M., 2003. A key role for TRPM7 channels in anoxic neuronal death. Cell 115, 863–877.

Aicher, W.K., Bühring, H.J., Hart, M., Rolauffs, B., Badke, A., Klein, G., 2011. Regeneration of cartilage and bone by defined subsets of mesenchymal stromal cells-potential and pitfalls. Adv. Drug Deliv. Rev. 63, 342–351.

Albert, A.P., Pucovský, V., Prestwich, S.A., Large, W.A., 2006. TRPC3 properties of a native constitutively active Ca^{2+}-permeable cation channel in rabbit ear artery myocytes. J. Physiol. 571, 361–369.

Bae, C.Y.J., Sun, H.-S., 2011. TRPM7 in cerebral ischemia and potential target for drug development in stroke. Acta Pharmacol. Sin. 32, 725–733.

Baron, A., Schaefer, L., Lingueglia, E., Champigny, G., Lazdunski, M., 2001. Zn^{2+} and H^{+} are coactivators of acid-sensing ion channels. J. Biol. Chem. 276, 35361–35367.

Bevan, S., Szolcsányi, J., 1990. Sensory neuron-specific actions of capsaicin: mechanisms and applications. Trends Pharmacol. Sci. 11, 331–333.

Bomben, V.C., Sontheimer, H.W., 2008. Inhibition of transient receptor potential canonical channels impairs cytokinesis in human malignant gliomas. Cell Prolif. 41, 98–121.

Cheng, H., Feng, J.M., Figueiredo, M.L., Zhang, H., Nelson, P.L., Marigo, V., Beck, A., 2010. Transient receptor potential melastatin type 7 channel is critical for the survival of bone marrow derived mesenchymal stem cells. Stem Cells Dev. 19, 1393–1403.

Chomczynski, P., Sacchi, N., 1987. Single-step method of RNA isolation by acid guanidinium thiocyanate–phenol–chloroform extraction. Anal. Biochem. 162, 156–159.

Chu, X.P., Xiong, Z.G., 2012. Physiological and pathological functions of acid-sensing ion channels in the central nervous system. Curr. Drug Targets 13, 263–271.

Clapham, D.E., 2003. TRP channels as cellular sensors. Nature 426, 517–524.

Cui, N., Zhang, X., Tadepalli, J.S., Yu, L., Gai, H., Petit, J., Pamulapati, R.T., Jin, X., Jiang, C., 2011. Involvement of TRP channels in the CO_2 chemosensitivity of locus coeruleus neurons. J. Neurophysiol. 105, 2791–2801.

Elizondo, M.R., Arduini, B.L., Paulsen, J., MacDonald, E.L., Sabel, J.L., Henion, P.D., 2005. Defective skeletogenesis with kidney stone formation in dwarf zebrafish mutant for TRPM7. Curr. Biol. 15, 667–671.

Grimm, C., Kraft, R., Schultz, G., Harteneck, C., 2005. Activation of the melastatin-related cation channel TRPM3 by d-erythro-sphingosine. Mol. Pharmacol. 67, 798–805.

Gunthorpe, M.J., Benham, C.D., Randall, A., Davis, J.B., 2002. The diversity in the vanilloid (TRPV) receptor family of ion channels. Trends Pharmacol. Sci. 23, 183–191.

Immke, D.C., McCleskey, E.W., 2003. Protons open acid-sensing ion channels by catalyzing relief of Ca^{2+} blockade. Neuron 37, 75–84.

Jetti, S.K., Swain, S.M., Majumder, S., Chatterjee, S., Poornima, V., Bera, A.K., 2010. Evaluation of the role of nitric oxide in acid sensing ion channel mediated cell death. Nitric Oxide 22, 213–219.

Jiang, X., Newell, E.W., Schlichter, L.C., 2003. Regulation of a TRPM7-like current in rat brain microglia. J. Biol. Chem. 278, 42867–42876.

Jiang, J., Li, M., Yue, L., 2005. Potentiation of TRPM7 inward current by protons. J. Gen. Physiol. 126, 135–150.

Kerschbaum, H.H., Kozak, J.A., Cahalan, M.D., 2003. Polyvalent cationsas permeant probes of MIC and TRPM7 pores. Biophys. J. 84, 2293–2305.

Leonardi, E., Ciapetti, G., Baglio, S.R., Devescovi, V., Baldini, N., Granchi, D., 2009. Osteogenic propwrties of late adherent subpopulations of human bone marrow stromal cells. Histochem. Cell Biol. 132 (5), 547–557.

Li, G.R., Deng, X.L., 2011. Functional ion channels in stem cells. World J. Stem Cells 3, 19–24.

Lingueglia, E., De Weille, J.R., Bassilana, F., Heurteaux, C., Sakai, H., Waldmann, R., Lazdunski, M., 1997. A modulatory subunit of acid sensing ion channels in brain and dorsal root ganglion cells. J. Biol. Chem. 272, 29778–29783.

Liu, Z.J., Zhuge, Y., Velazquez, O.C., 2009. Trafficking and differentiation of mesenchymal stem cells. J. Cell. Biochem. 106 (6), 984–991.

Nadler, M.J.S., Hermosura, M.C., Inabe, K., Perraud, A.L., Zhu, Q., Stokes, A.J., Kurosaki, T., Kinet, J.-P., Penner, R., Scharenberg, A.M., Fleig, A., 2001. LTRPC7 is a Mg.ATP-regulated divalent cation channel required for cell viability. Nature 411, 590–595.

Nakayama, G.R., Caton, M.C., Nova, M.P., Parandoosh, Z., 1997. Assessment of the Alamar Blue assay for cellular growth and viability in vitro. J. Immunol. Methods 204, 205–208.

Nedergaard, M., Kraig, R.P., Tanabe, J., Pulsinelli, W.A., 1991. Dynamics of interstitial and intracellular pH in evolving brain infarct. Am. J. Physiol. 260, 581–588.

Paukert, M., Babini, E., Pusch, M., Gründer, S., 2004. Identification of the Ca^{2+} blocking site of acid-sensing ion channel (ASIC) 1: implications for channel gating. J. Gen. Physiol. 124, 383–394.

Peter, H., 2007. Role of visceral afferent neurons in mucosal inflammation and defense. Curr. Opin. Pharmacol. 7, 563–569.

Romero-Mendez, A.C., Algara-Suarez, P., Sanchez-Armass, S., Mandeville, P.B., Meza, U., Espinosa-Tanguma, R., 2008. Intracellular Ca^{2+}-store depletion triggers a Na^{+} influx via SOCs in guinea pig tracheal smooth muscle. FASEB J. 22, 1206.1201.

Semtner, M., Schaefer, M., Pinkenburg, O., Plant, T.D., 2007. Potentiation of TRPC5 by protons. J. Biol. Chem. 282, 33868–33878.

Siesjo, B.K., Katsura, K., Kristian, T., 1996. Acidosis-related damage. Adv. Neurol. 71, 209–233 (discussion 234–236).

Sreejit, P., Verma, R.S., 2011. Cardiogel supports adhesion, proliferation and differentiation of stem cells with increased oxidative stress protection. Eur. Cell. Mater. 21, 107–121.

Staruschenko, A., Dorofeeva, N.A., Bolshakov, K.V., Stockand, J.D., 2007. Subunit-dependent cadmium and nickel inhibition of acid-sensing ion channels. Dev. Neurobiol. 67, 97–107.

Sugiura, T., Bielefeldt, K., Gebhart, G.F., 2007. Mouse colon sensory neurons detect extracellular acidosis via TRPV1. Am. J. Physiol. Cell Physiol. 292, C1768–C1774.

Tousova, K., Vyklicky, L., Susankova, K., Benedikt, J., Vlachova, V., 2005. Gadolinium activates and sensitizes the vanilloid receptor TRPV1 through the external protonation sites. Mol. Cell. Neurosci. 30, 207–217.

Ullrich, N.D., Voets, T., Prenen, J., Vennekens, R., Talavera, K., Droogmans, G., Nilius, B., 2005. Comparison of functional properties of the Ca^{2+}-activated cation channels TRPM4 and TRPM5 from mice. Cell Calcium 37, 267–278.

Voets, T., Droogmans, G., Wissenbach, U., Janssens, A., Flockerzi, V., Nilius, B., 2004. The principle of temperature-dependent gating in cold- and heat-sensitive TRP channels. Nature 430, 748–754.

Wei, C., Wang, X., Chen, M., Ou-Yang, K., Song, L.S., Cheng, H., 2009. Calcium flickers steer cell migration. Nature 457, 901–905.

Xiong, Z.-G., Zhu, X.M., Chu, X.P., Minami, M., Hey, J., Wei, W.L., MacDonald, J.F., Wemmie, J.A., Price, M.P., Welsh, M.J., Simon, R.P., 2004. Neuroprotection in ischemia: blocking calcium-permeable acid-sensing ion channels. Cell 118, 687–698.

Zhao, S., Wehner, R., Bornhauser, M., Wassmuth, R., Bachmann, M., Schmitz, M., 2010. Immunomodulatory properties of mesenchymal stromal cells and their therapeutic consequences for immune-mediated disorders. Stem Cells Dev. 19, 607–614.